Electronic Supplementary Material (ESI) for Journal of Materials Chemistry A.

Supporting Information

Regulating the Interlayer Spacing of $Ca_{0.55}ZrH_{0.9}(PO_4)_2$ for Selective Removal of Sr^{2+} from Acidic Wastewater

Ruixi Liu,[ab] Qian Zhao,[ab] Zeru Wang,[ab] Rui Jiang,[ab] Chuancong Lin,[ab] LinZhen Wu,[ab] Guangyuan Chen,[ab] Pan He,[ab] Lin Zhu,*[ab] Jing Chen,*[c] Tao Duan*[ab]

[a] National Co-Innovation Center for Nuclear Waste Disposal and Environmental Safety, Southwest University of Science and Technology, Mianyang 621010, China.

[b] State Key Laboratory of Environment-friendly Energy Materials, Key Laboratory of Solid Waste Treatment and Resource Recycle, Ministry of Education, Southwest University of Science and Technology, Mianyang 621010, China.

[c] Institute of Nuclear and New Energy Technology, Tsinghua University, Beijing 100084, China

* Corresponding Author：

(Lin Zhu) Email: zhulin@swust.edu.cn

(Jing Chen) Email: jingxia@mail.tsinghua.edu.cn

(Tao Duan) Email: duant@ustc.edu.cn

1. Isothermal adsorption experiments and kinetic experiments. In the batch adsorption experiment, the solid-liquid ratio was 1:2 (adsorbent 5mg, 10ml solution). The pH value of the solution was adjusted by a certain amount of HNO_3 and NaOH, which did not affect the concentration of the solution. The pH of the solution was also monitored by a pH meter.

In summary, 5 mg of the adsorbent was added to a 10 mL solution containing Sr and stirred for 12 hours on a constant-temperature magnetic stirrer. The solution was then separated and filtered using a 0.22 μm nylon membrane filter. The concentration of Sr^{2+} in the supernatant was analyzed using ICP-MS. By measuring the difference in Sr^{2+} concentration in the solution before and after adsorption, the equilibrium adsorption capacity was calculated using the following formula:

$$q_e = \frac{(C_0 - C_e) \times V}{M} \qquad \text{(S1)}$$

where C_0 (mg·L^{-1}) is the initial concentration of metal ions, Ce (mg·L^{-1}) is the equilibrium concentration, V (L) is the volume of the test solution and M (g) is sorbent dose.

The removal rate of material can be calculated by the following formula:

$$Removal\ rate(\%) = \frac{(C_0 - C_e)}{C_0} \text{x } 100\% \qquad \text{(S2)}$$

where C_0 and C_e represent the initial and equilibrium concentrations of Sr^{2+} or Cs^+, respectively.

2. Competing Ion Experiment Procedure. 5 mg of the material was added to a pre-prepared solution and stirred for 12 hours on a constant-temperature magnetic stirrer. The solution was then separated and filtered using a 0.22 μm nylon membrane filter.

The concentrations of Sr^{2+}, Cs^{+}, La^{3+}, and other metal ions in the clear solution were analyzed using ICP-MS.

The Sr^{2+}, Cs^{+}, and La^{3+} systems were prepared in ratios of 1:1:1, 1:5:5, and 1:10:10, respectively. The corresponding ion concentrations in these systems were 10 ppm:10 ppm:10 ppm, 10 ppm:50 ppm:50 ppm, and 10 ppm:100 ppm:100 ppm. The competition system concentration ratio of Sr^{2+} to other metal ions was 10 ppm:100 ppm.

3.Distribution coefficient (Kd). The distribution coefficient Kd value can be calculated by the following formula:

$$K_d = \frac{V}{m} \times \frac{(C_0 - C_e)}{C_e} \tag{S3}$$

where C_0 (mg/L) and C_e (mg/L) are the initial and equilibrium concentrations of the target ion, respectively; m (g) and V (mL) are the mass of the ion exchange material and the volume of the solution used in the ion exchange experiment respectively.

4.The adsorption data fitting by isotherm models. The Langmuir isotherm model and the Freundlich isotherm model can be expressed by the eq 3 and eq 4.

$$\ln q_e = \ln K_F + n \ln C_e \tag{S4}$$

$$\frac{C_e}{q_e} = \frac{C_e}{q_m} + \frac{1}{q_m K_L} \tag{S5}$$

For both equations, q_e (mg/g) and q_m (mg/g) are the adsorption capacity at equilibrium and saturation adsorption capacity, respectively; Ce (mg/L) is the Sr^{2+} concentration in the solution at equilibrium; K_L and K_F are the Langmuir and Freundlich constant, respectively.

5.The adsorption data fitting by kinetic models. The pseudo-first-order and pseudo-second-order models can be expressed by the eq 5 and eq 6.

$$q_t = q_e - e^{lnq_e - tk_1} \tag{S6}$$

$$q_t = \frac{t}{\frac{1}{k_2 q_e^2} + \frac{t}{q_e}} \tag{S7}$$

For both equations, where q_t (mg/g) is the amount of uranium adsorbed at time t (h), q_e (mg/g) is the amount of uranium adsorbed at equilibrium, k_1(min^{-1}) represents the rate constant of pseudo-first-order kinetic model, and k_2 (g mg^{-1} min^{-1}) represents the rate constant of pseudo-second-order kinetic model.

6. Bragg's law formula.

$$d = \frac{\lambda}{2Sin\frac{2\theta}{2}} \tag{S8}$$

Here, λ is the X-ray wavelength during XRD analysis, and 2θ (◦) is the position of the Bragg diffraction peak in the XRD pattern.

7. Theoretical calculation methods. The theoretical calculations in this study were performed using the VASP (Vienna Ab initio Simulation Package) software, and the overall research is based on Density Functional Theory (DFT), employing the plane-wave pseudopotential method. The Generalized Gradient Approximation (GGA) with the Projector Augmented Wave (PAW) method was used to describe the interaction between ions and electrons, and the Perdew-Burke-Ernzerhof (PBE) functional was used to describe the electron exchange-correlation interaction. The plane-wave cutoff energy was uniformly set to 520 eV. The Brillouin zone k-point mesh was generated using the Monkhorst-Pack method, with a k-point grid set to 4×6×3. During the calculations, the convergence criteria for the total energy were set to 1×10^(-5) eV, and the convergence criteria for the single atomic forces were set to -0.02 eV/Å. The adsorption energy is typically calculated using the following formula:

$$E_{ads} = E_{total} - E_{Zrp} - E_{Ca^{2+}} \tag{S9}$$

$$E_{ads} = E_{total} - E_{Zrp} - E_{Sr^{2+}} \tag{S10}$$

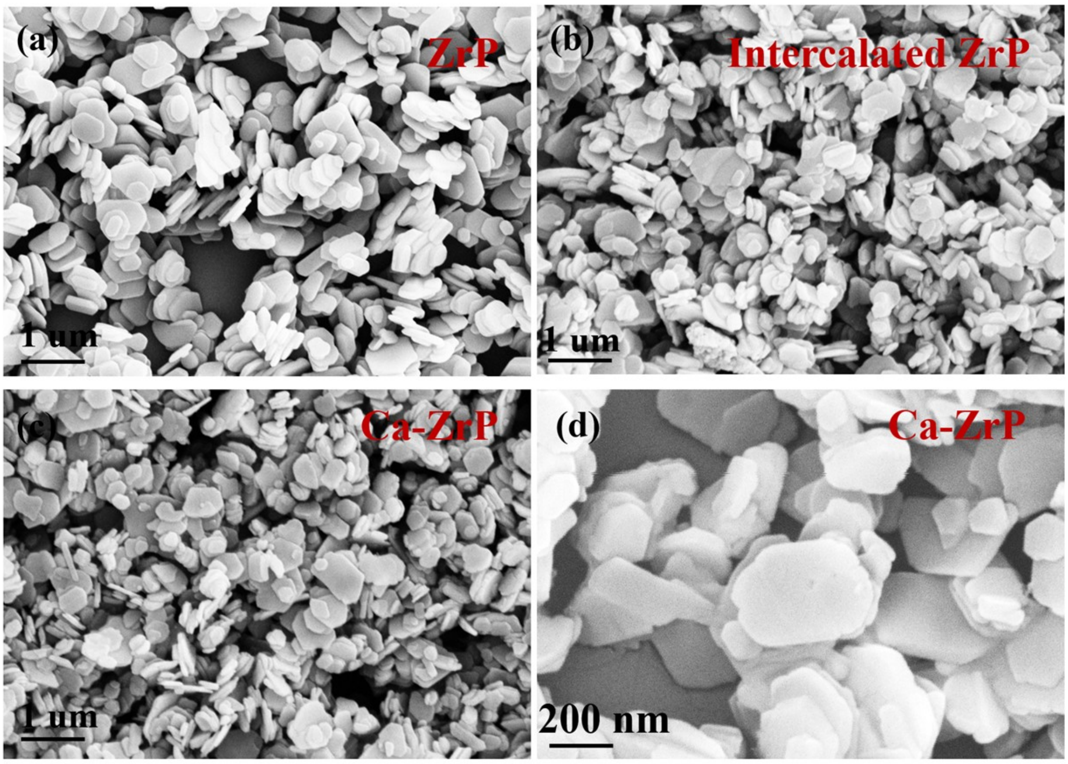

Fig. S1 (a)~(d) show the SEM images of ZrP, intercalated ZrP and Ca-ZrP respectively.

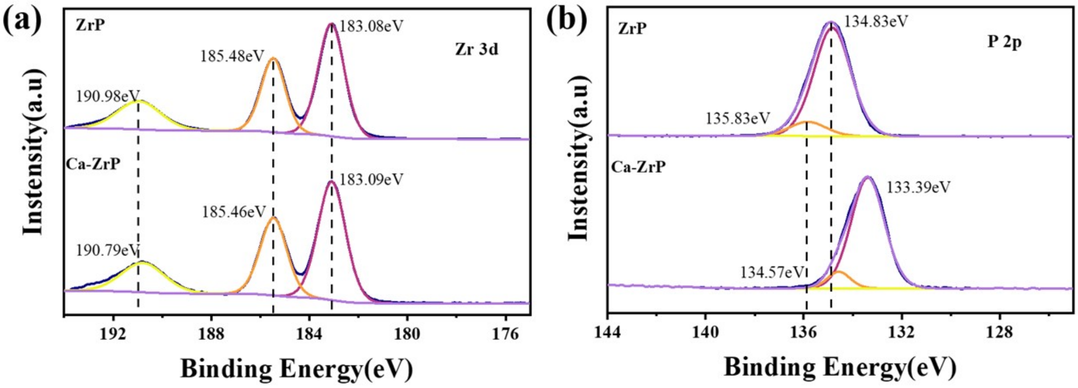

Fig. S2 (a) Comparison of the Zr 3d characteristic peaks of original ZrP and Ca-ZrP; (b) Comparison of the P 2p characteristic peaks of original ZrP and Ca-ZrP;

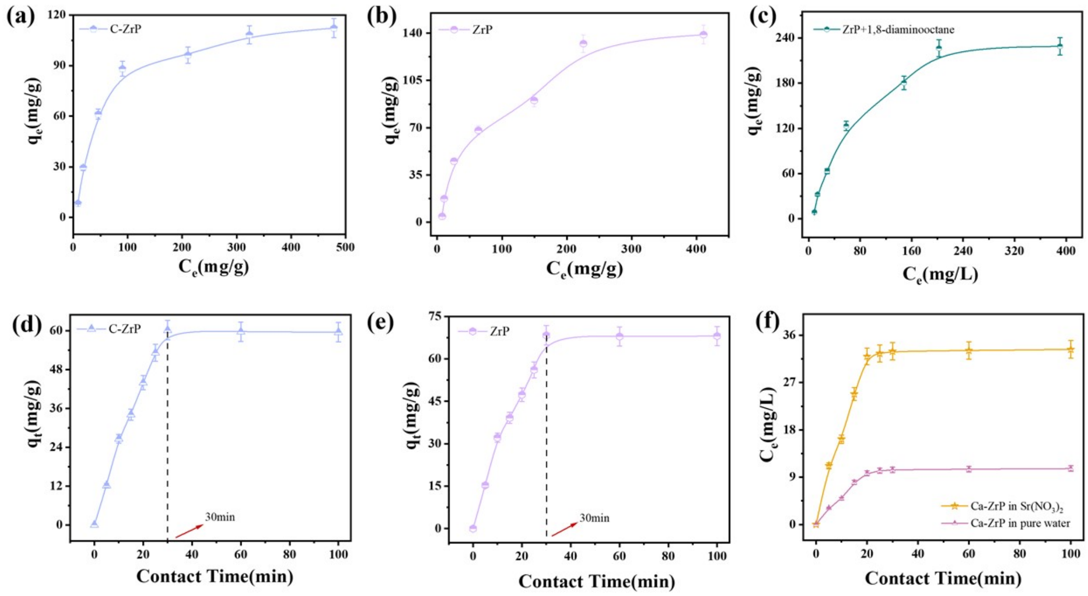

Fig. S3 (a) and (b) show the Sr^{2+} adsorption capacity of commercial ZrP and hydrothermal ZrP respectively; (c) shows the capacity of ZrP to capture Sr^{2+} after intercalation; (d)) and (e) are the kinetic spectra of Sr^{2+} adsorption by commercial ZrP and hydrothermal ZrP respectively. (f) shows the comparison of the Ca^{2+} precipitation amount of Ca-ZrP in $Sr(NO_3)_2$ and pure water respectively;

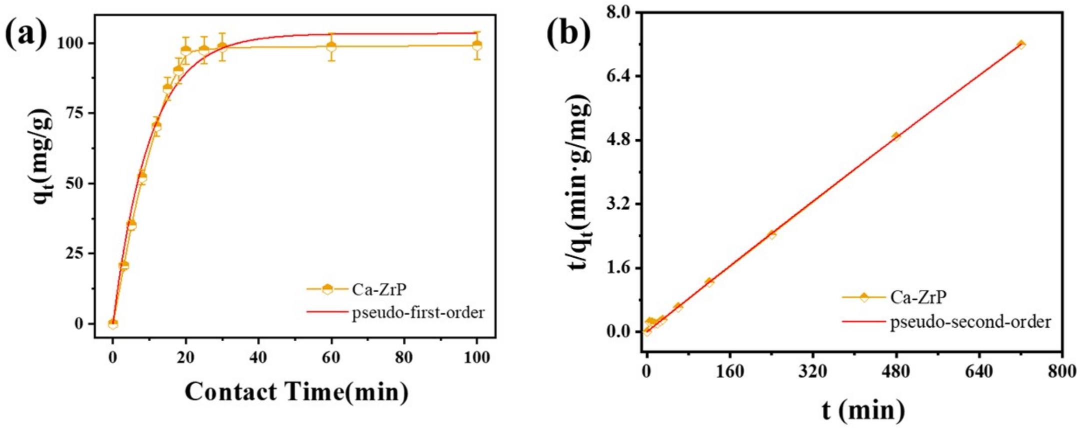

Fig. S4 (a) P pseudo-first-order kinetic model fitting diagram of the kinetic data of Sr^{2+} captured by Ca-ZrP in neutral solution; (b) P pseudo-first-order kinetic model fitting of kinetic data of Sr^{2+} captured by Ca-ZrP in neutral solution Second-order kinetic model fitting chart;

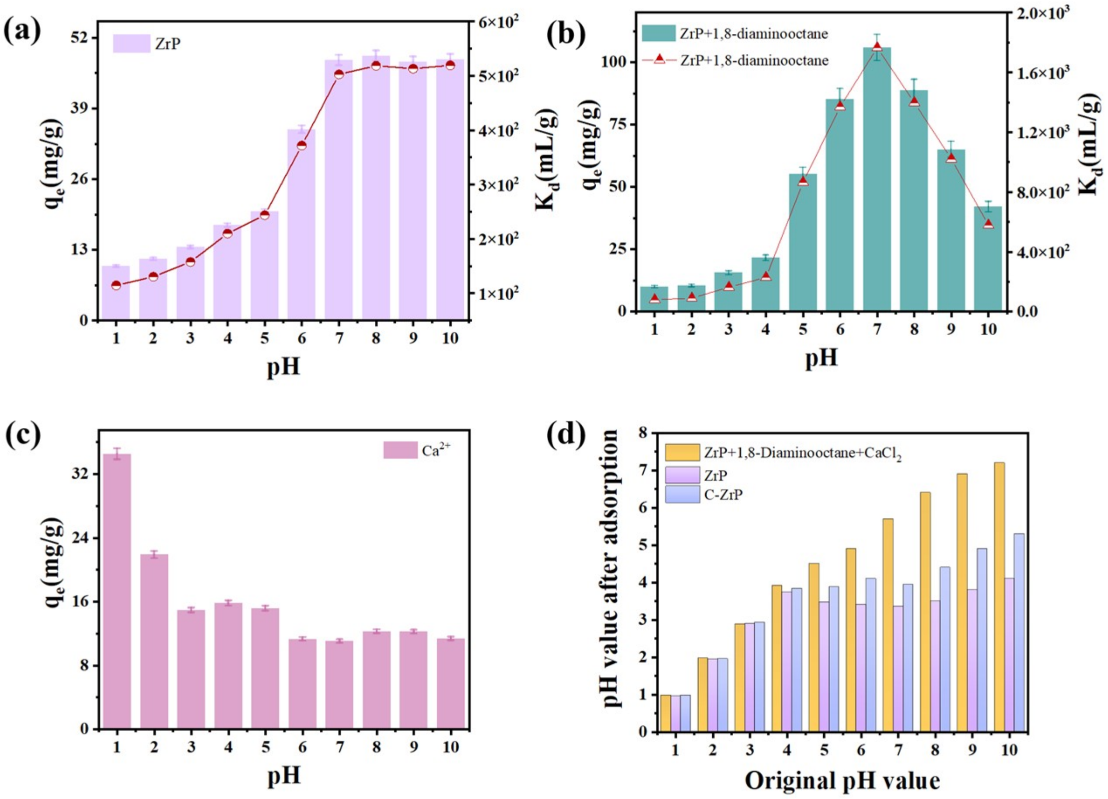

Fig. S5 (a) and (b) show the capacity and Kd values for trapping Sr^{2+} as a function of pH for hydrothermally prepared ZrP and ZrP after intercalation, respectively.; (c) shows the amount of Ca^{2+} precipitated when Ca-ZrP traps Sr^{2+} with pH change; and (d) shows the pH change of Ca-ZrP, C-ZrP, and ZrP before and after the experiment. (e) shows the XRD pattern of Ca-ZrP before and after irradiation.

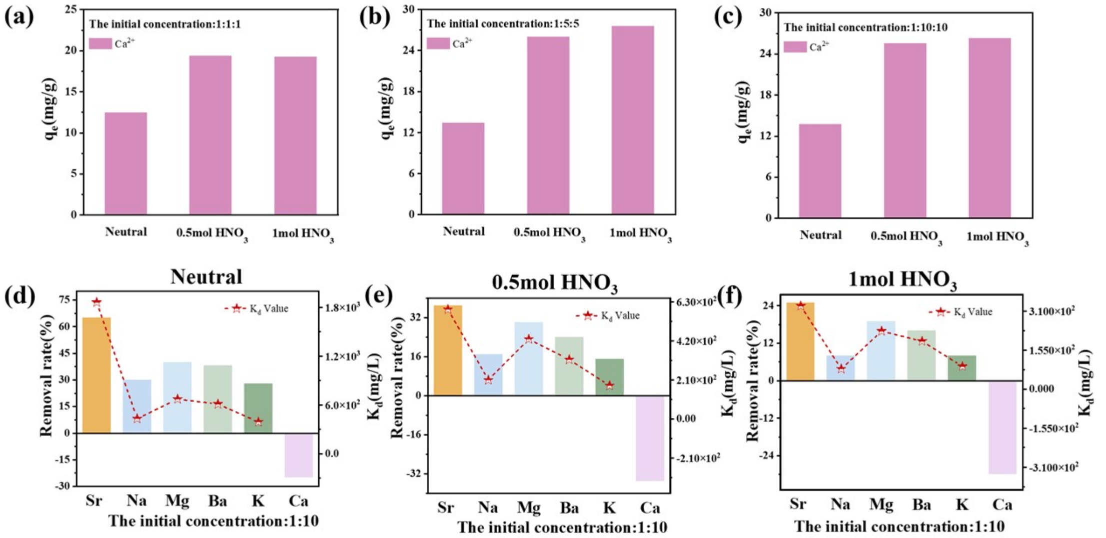

Fig. S6. (a), (b), and (c) respectively show the Ca^{2+} precipitation capacity of Ca-ZrP in neutral, 0.5 mol/LHNO_3, and 1 mol/LHNO_3 solutions under different initial competing ion ratios. The pictures (d), (e), and (f) respectively show the removal of each ion by Ca-ZrP in neutral, 0.5mol/LHNO_3, and 1mol/LHNO_3 solutions at the initial ratio of Sr/other metals of 1:10. rates and correlation coefficients.

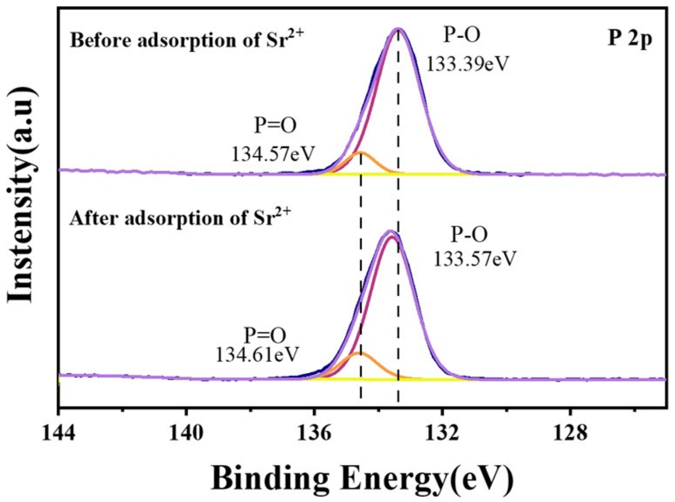

Fig S7: High-resolution XPS region of P 2p.

Table S1. Parameters for Isotherm Models of Sr^{2+} adsorption on Ca-ZrP.

Samples	Langmuir constant			Freundlich constant		
	q_m(mg/g)	K_L(L/mg)	R^2	n	K_F(mg/g)	R^2
Ca-ZrP	226.9	0.01	0.99	2.94	9.96	0.92

Table S2. Kinetic parameters of Sr^{2+} capture by CA@ZrP (90%) and ZrP

Samples	Pseudo-first-order			Pseudo-second-order		
	q_e(mg/g)	K_1(min^{-1})	R^2	q_e(mg/g)	K_2(g/mg min^{-1})	R^2
Ca-ZrP	100.13	1.07	0.98	100.13	9.45×10^{-7}	0.99

Table S3. The adsorption performance of C-ZrP 、ZrP and Ca-ZrP with other similar adsorbents for Sr^{2+} was compared.

Adsorbents	pH	Equilibrium time (min)	Adsorption capacity (mg/g)	References
TMP-MS	---	60	68	[1]
Porous	11	14	45.36	[2]
Hydroxyapatite	---	---	---	---
Zr–Mn oxide/PAN	8	222	21.37	[3]
Na_2TinO_{2n+1}/SiO_2	8	5	33.31	[4]
Sodium trititanate	6	＞500	85.26	[5]
PAN-zeolite	7	90	98.13	[6]
Natural zeolite	8	---	1.3	[7]
CHA-type zeolite	7	---	9.7	[8]
Pecan shell-based AC	7	---	8.8	[9]
Commercial AC	4	---	4.4	[10]
K-NGH-1	7		41.62	[11]
FJSMSnS-2	7		59.41	[12]
FJSM-SnS-4	7		147	[13]
C-ZrP	7	240	112.2	This Work
ZrP	7	240	138.9	This Work
Ca-ZrP	7	240	226.9	This Work

Table S4. Adsorption of Sr^{2+} by different materials in low pH environment.

	pH	Adsorption capacity (mg/g)	References
Hex-WO_3	2	21	[14]
TiO_2-PAN	2	9	[15]
ZnO	4	20	[16]
CaO NPs@MOF-5	2	1.2	[17]
Activated carbon	2	3.7	[10]
C-ZrP	1	5.1	This Work
ZrP	1	9.9	This Work
Ca-ZrP	1	34.5	This Work

Table S5. Parameters for capturing each ion of Ca-ZrP at room temperature in neutral, 0.5mol/L HNO_3, 1mol/L HNO_3 environments with an initial ratio of Sr/Cs/La of 1:1:1.

C_0^{Sr} mg/L	C_0^{Cs} mg/L	C_0^{La} mg/L	C_e^{Sr} mg/L	C_e^{Cs} mg/L	C_e^{La} mg/L	R^{Sr} %	K_d^{Sr} mL/g	R^{Cs} %	K_d^{Cs} mL/g	R^{La} %	K_d^{La} mL/g
Neutral											
9.899	10.12	9.869	1.782	6.982	5.724	82	4.56×10^3	30	0.3×10^3	42	0.72×10^3
0.5mol/L HNO_3											
10.08	10.07	9.817	4.032	8.679	7.559	60	1.01×10^3	13	0.16×10^3	23	0.30×10^3
1mol/L HNO_3											
10.05	10.85	9.917	5.628	10.09	8.778	44	0.79×10^3	7	0.08×10^3	13	0.15×10^3

Table S6. Parameters for capturing each ion of Ca-ZrP at room temperature in neutral, 0.5mol/L HNO_3, 1mol/L HNO_3 environments with an initial ratio of Sr/Cs/La of 1:5:5.

C_0^{Sr} mg/L	C_0^{Cs} mg/L	C_0^{La} mg/L	C_e^{Sr} mg/L	C_e^{Cs} mg/L	C_e^{La} mg/L	R^{Sr} %	K_d^{Sr} mL/g	R^{Cs} %	K_d^{Cs} mL/g	R^{La} %	K_d^{La} mL/g
Neutral											
10.49	50.89	49.72	2.37	39.19	30.83	78	3.45×10^3	23	0.30×10^3	38	0.61×10^3
0.5mol/L HNO_3											
9.98	49.86	50.82	5.79	44.87	40.15	42	0.72×10^3	10	0.11×10^3	21	0.27×10^3
1mol/L HNO_3											
9.65	50.85	49.13	6.66	48.30	43.73	31	0.45×10^3	5	0.05×10^3	11	0.12×10^3

Table S7. Parameters for capturing each ion of Ca-ZrP at room temperature in neutral, 0.5mol/L HNO_3, 1mol/L HNO_3 environments with an initial ratio of Sr/Cs/La of 1:10:10.

C_0^{Sr} mg/L	C_0^{Cs} mg/L	C_0^{La} mg/L	C_e^{Sr} mg/L	C_e^{Cs} mg/L	C_e^{La} mg/L	R^{Sr} %	K_d^{Sr} mL/g	R^{Cs} %	K_d^{Cs} mL/g	R^{La} %	K_d^{La} mL/g
Neutral											
9.83	100.39	100.71	2.75	82.32	74.52	72	2.57×10^3	18	0.22×10^3	26	0.35×10^3
0.5mol/L HNO_3											
9.88	99.86	100.82	6.13	90.87	86.7	38	0.61×10^3	9	0.09×10^3	14	0.16×10^3
1mol/L HNO_3											
9.85	100.15	99.33	7.19	97.15	90.39	27	0.37×10^3	3	0.03×10^3	9	0.10×10^3

Table S8. Parameters for capturing each ion of Ca-ZrP at room temperature in a neutral, 0.5mol/L HNO_3, 1mol/L HNO_3 environment, with an initial ratio of Sr/other metals of 1:10.

C_0^{Sr} mg/L	C_0^{Na} mg/L	C_0^{Mg} mg/L	C_0^{Ba} mg/L	C_0^{K} mg/L	C_0^{Ca} mg/L	R^{Sr} %	K_d^{Sr} mL/g	R^{Na} %	K_d^{Na} mL/g	R^{Mg} %	K_d^{Mg} mL/g	R^{Ba} %	K_d^{Ba} mL/g	R^{K} %	K_d^{K} mL/g	R^{Ca} %	K_d^{Ca} mL/g
Neutral																	
9.82	98.32	99.53	100.2	100.1	98.32	65	1.86×10^3	30	0.43×10^3	40	0.67×10^3	38	0.61×10^3	28	0.39×10^3	-25	----
0.5mol/L HNO_3																	
9.92	97.38	100.5	97.21	99.76	99.14	37	0.59×10^3	17	0.21×10^3	30	0.43×10^3	24	0.32×10^3	15	0.18×10^3	-35	----
1mol/L HNO_3																	
9.92	99.18	98.32	97.91	100.2	98.62	25	0.33×10^3	8	0.08×10^3	19	0.23×10^3	16	0.19×10^3	8	0.09×10^3	-30	----

Table S9. Removal rates of Sr^{2+} by different materials in competing ionic environments.

Competitive ion environment		Removal rate (%)	K_d(ml/g)	References
Na_2TinO_{2n+1}/SiO_2	Mg、K、Na、Ca、Cs	---	＞1x10^4	[4]
$NH_4V_4O_{10}$	Na、K、Al、Ca、Gu	---	＞3x10^2	[18]
multi-walled-carbon nanotube	Na、K、Mg、Ca、Cs	---	2.919	[19]
P-MWCNT	Na、K、Mg、Ca、C	---	4.140	[19]
Ca-ZrP	Na、K、Mg、Ca、Ba	65	1.86x10^3	This Work

Table S10. The ratio of each element in Ca-ZrP before adsorption.

Peak Table:	Name	Start BE	Peak BE	End BE	Area(P)CPS.eV	Area(N)TPP-2M	Atomic%
	C1s	297.98	284.6	279.18	81796.71	1146.84	16.72
	Ca2p	359.98	347.64	340.18	231097.37	565.61	8.25
	O1s	544.98	531.33	525.18	658907.79	3820.73	55.71
	P2p	143.98	133.4	124.18	96282.85	910.49	13.28
	Zr3d	193.98	183.08	174.18	284227	414.46	6.04

Table S11. Ratio of each element in Ca-ZrP after adsorption of Sr^{2+}.

Peak Table:	Name	Start BE	Peak BE	End BE	Area(P)CPS.eV	Area(N)TPP-2M	Atomic%
	C1s	297.98	284.62	279.18	59117.01	828.87	10.96
	Ca2p	359.98	347.73	340.18	196036.22	479.82	6.35
	O1s	544.98	531.48	525.18	772618.21	4480.62	59.27
	P2p	143.98	133.65	124.18	114372.92	1081.71	14.31

Sr3d	141.98	133.61	126.18	113210.23	201.85	2.67
Zr3d	193.98	183.24	174.18	333550.08	486.43	6.43

References

1 A. R. Khanchi, *Appl. Surf. Sci.*, 2012.

2 X. Xia, J. Shen, F. Cao, C. Wang, M. Tang, Q. Zhang and S. Wei, *Journal of Hazardous Materials*, 2019, **368**, 326-335.

3 S. İnan and Y. Altaş, *Chem. Eng. J.*, 2011, **168**, 1263-1271.

4 C. Liu, L. Chen, Z. Ye, C. Li, X. Yin, X. Wang and Y. Wei, *Journal of Sol-Gel Science and Technology*, 2019, **91**, 273-285.

5 W. Guan, J. Pan, H. Ou, X. Wang, X. Zou, W. Hu, C. Li and X. Wu, *Chem. Eng. J.*, 2011, **167**, 215-222.

6 H. Faghihian, M. Iravani, M. Moayed and M. Ghannadi-Maragheh, *Chem. Eng. J.*, 2013, **222**, 41-48.

7 T. Abdollahi, J. Towfighi and H. Rezaei-Vahidian, *Environ. Technol. Innovation*, 2020, **17**, 100592.

8 J. Liang, J. Li, X. Li, K. Liu, L. Wu and G. Shan, *Sep. Purif. Technol.*, 2020, **230**, 115874.

9 A. R. Kaveeshwar, P. S. Kumar, E. D. Revellame, D. D. Gang, M. E. Zappi and R. Subramaniam, *J. Cleaner Prod.*, 2018, **193**, 1-13.

10 S. Chegrouche, A. Mellah and M. Barkat, *Desalination*, 2009, **235**, 306-318.

11 H. Sun, B. Hu, T. Lv, Y. Guo, Y. X. Yao, L. Yang, M. Feng and X. Huang, *Small*, 2023, e2208212.

12 W.-A. Li, J.-R. Li, B. Zhang, H.-Y. Sun, J.-C. Jin, X.-Y. Huang and M.-L. Feng, *ACS Appl. Mater. Interfaces*, 2021, **13**, 10191-10201.

13 J. Li, J. Jin, T. Zhang, W. Ma, X. Zeng, H. Sun, M. Cheng, M. Feng and X. Huang, *ACS ES&T Water*, 2021.

14 X. Li, W. Mu, X. Xie, B. Liu, H. Tang, G. Zhou, H. Wei, Y. Jian and S. Luo, *J. Hazard. Mater.*, 2014, **264**, 386-394.

15 S. Kasap, H. Tel and S. Piskin, *J. Radioanal. Nucl. Chem.*, 2011, **289**, 537-544.

16 Ü. H. Kaynar and S. Ç. Kaynar, *Celal Bayar University Journal of Science*, 2017, **13**, 185-191.

17 S. Yekta and M. Sadeghi, *J. Inorg. Organomet. Polym. Mater.*, 2018, **28**, 1049-1064.

18 H. Zhang, C. Li, X. Chen, H. Fu, Y. Chen, S. Ning, T. Fujita, Y. Wei and X. Wang, *J. Colloid. Interface. Sci.*, 2022, **615**, 110-123.

19 S. Ali, I. A. Shah and H. Huang, *Sep. Purif. Technol.*, 2020, **237**, 116352.